Triple electron capture in fast 0.5–1.1 MeV/u C^{6+} on Ar collisions

M. Zamkov, E. P. Benis,* P. Richard, and T. G. Lee
James R. Macdonald Laboratory, Department of Physics, Kansas State University, Manhattan, Kansas 66506-2604

T. J. M. Zouros
Department of Physics, University of Crete, P. O. Box 2208, 71003 Heraklion, Crete, Greece
and Institute of Electronic Structure and Laser, P. O. Box 1527, 71110, Heraklion, Crete, Greece
(Received 21 May 2002; published 22 October 2002)

Doubly excited *KLL* states were populated by triple electron capture in collisions of fast ($v = 4.5–6.6$ a.u.) C^{6+} ions with Ar atoms. Measurements of the Auger-electron emission in the direction of the ion beam were used to determine the absolute single differential cross sections for the triple electron capture to all autoionizing *KLL* states. The results were compared with cross sections calculated within the independent-particle model, in which the simultaneous capture of all three target electrons was assumed. Single electron capture probabilities, employed by the model, were calculated using the two-center semiclassical close-coupling method, based on an atomic orbital expansion. In order to allow comparison of the measured zero-degree differential cross sections with calculated total cross sections, the Auger-electron emission from the doubly excited *KLL* states was assumed isotropic. Model calculations were found to be in a good agreement with the experimental data. An adequate description of the triple electron capture by the model implies that the projectile screening and electron-electron correlation effects in multiple electron capture are significantly reduced in fast, highly charged ion-atom collisions.

DOI: 10.1103/PhysRevA.66.042714 PACS number(s): 34.70.+e, 34.50.Fa

I. INTRODUCTION

Multiple electron capture in collisions of highly charged ions with multielectron atoms or molecules has become a very active area of atomic physics research in the last decade. Transfer processes with more than two active electrons represent a fundamental problem of a many-body dynamic system, thus providing tests for most contemporary atomic models. The present understanding of multiple electron transfer has come from numerous experimental and theoretical studies primarily in terms of the classical quasimolecular description of the process. To date, however, a unified treatment that accounts for a wide range of energies has not yet come forth. In particular, the role of electron-electron correlation effects in multielectron capture still remains unclear, raising the demand for a more comprehensive model.

The investigation of multiple electron transfer processes has been stimulated by the introduction of more advanced ion sources during the 1980s, as attested by a number of experimental publications [1–7]. Projectile charge-change, recoil-ion production, and total charge-transfer [1–4,8,9] cross sections were obtained for collisions of Ar^{q+}, I^{q+}, and Xe^{q+} projectiles with various targets. Triple electron capture stabilization ratios were investigated by measuring the visible photon emission from Rydberg transitions [5]. The Auger-electron spectroscopy was initially implemented in coincidence experiments with charge-state analyzed recoil ions [6,7] and then subsequently employed in time-of-flight (TOF) triple coincidence with scattered projectile and target ions to study collisions of O^{7+} and $^{15}N^{7+}$ with Ar gas targets [8,9]. The use of Auger-electron spectroscopy in ion-beam and ion-beam–recoil-ion experiments made it possible to account for the projectile or excited target charge change caused by the Auger decay following the collision. Thus, light elements, for which Auger decay is dominant, were included in the multielectron capture studies.

Theoretically, the quantum-mechanical or even semiclassical treatment of collision systems with more than two active electrons is generally a difficult task since a large number of reaction channels are involved. In view of that, the simple classical overbarrier model [10] was extended [11,12] to account for multielectron processes. Predictions of this model have been found to be in reasonable agreement with the experimental results. However, due to the fact that it ignores the electron-electron correlation and oversimplifies the electron transfer processes, the model could not give a precise description of multiple electron capture in slow collisions [13], whereas the breakdown of the first Born approximation at higher impact velocities ($v > 1$ a.u.) makes this representation inapplicable in the case of fast ion-atom collisions. An alternative treatment of multielectron transfer processes has been introduced by the independent electron model utilizing the uncorrelated Hartree-Fock approximation [14]. Although, the study was on double electron capture in $He^{2+} + He$ collisions at high impact velocities, it allows for the extension to systems with more than two electrons. Resulting in overall favorable agreement with experiment, this work indicated the diminishing role of the electron correlation effects at increasing impact velocities.

Experimental investigation of multiple electron transfer resulting from fast, highly charged ion-atom collisions is hampered by the rapid falloff of capture probabilities with increasing velocity of the ion. To the best of our knowledge, the study of true triple electron capture in fast ($v > 1$ a.u.) collisions has not yet been attempted experimentally. Mean-

*Email address: benis@phys.ksu.edu

while, the problem of multiple electron transfer at high impact velocities becomes more appealing, instigated by the dominant role of the process in populating lower-lying multiexcited states, recently a very dynamic area of atomic research. Additional incentives to investigate multielectron processes in fast collisions are provided by their importance in such diverse areas as high-temperature plasma studies, astrophysics, and laser technology.

As previously mentioned, the extended classical overbarrier (ECB) model cannot be utilized for predictions in fast ion-atom collisions, due to the fact that the interaction time at higher projectile velocities is not long enough for target electrons to be molecularized. However, since in fast ion-atom collisions projectile core states do not fully readjust due to the small interaction time, and are thus only partly screened by target electrons during the collision, greater confidence is given to the independent-particle model which includes the possibility of simultaneous capture of two or more electrons at similar internuclear distances.

The excited states of light projectiles decay mainly by emitting Auger electrons, thus favoring the use of Auger-electron spectroscopy. In addition, the very low probability of multielectron capture at high velocities necessitates the use of highly efficient spectrographs in such measurements.

In this work, high-resolution zero-degree Auger-electron projectile spectroscopy has been used to study triple electron capture to doubly excited *KLL* states of carbon in collisions of fast ($v=4.5$–6.6 a.u.) C^{6+} ions with Ar gas targets. Absolute single differential cross sections (SDCS's) have been obtained from the double differential cross section (DDCS) spectra and used to test the predictions of the independent-particle model, in which the simultaneous capture of all three target electrons is assumed. Single electron capture probabilities, employed by the model, were calculated using the two-center semiclassical close-coupling method [15], based on an atomic orbital expansion [16]. In order to allow comparison of the measured zero-degree differential cross sections with calculated total cross sections, Auger-electron emission from the doubly excited *KLL* states was assumed isotropic. Model calculations were found to be in good agreement with the experimental data. The influence of the present study on the understanding of projectile screening and electron-electron correlation effects in multiple electron capture is discussed.

II. EXPERIMENTAL PROCEDURE

The experiments were performed in the J. R. Macdonald Laboratory at Kansas State University, using the 7 MV EN tandem Van de Graaff accelerator. The C^{6+} beam was magnetically selected after colliding the primary Li-like C^{3+} beam with a $5\mu g/cm^2$ carbon foil, and then focused into a 5 cm long differentially pumped gas cell. In collisions with Ar atoms, doubly excited *KLL* states of C^{3+} ions were populated. These states decay dominantly by emitting Auger electrons at energies corresponding to the $1s^2\,{}^1S$ ground state transition. The Auger electrons emitted in the forward direction were detected with a zero-degree hemispherical spectrograph [17–19], capable of analyzing electrons in an energy bandwidth of about 20% of the mean pass energy, which significantly facilitates experimental measurements of low intensity processes, such as triple electron capture. The projectile beam current was measured by a Faraday cup, located at the exit aperture of the spectrograph, and the Auger-electron emission intensity was normalized to the integrated beam current. The experimental setup is shown in Fig. 1.

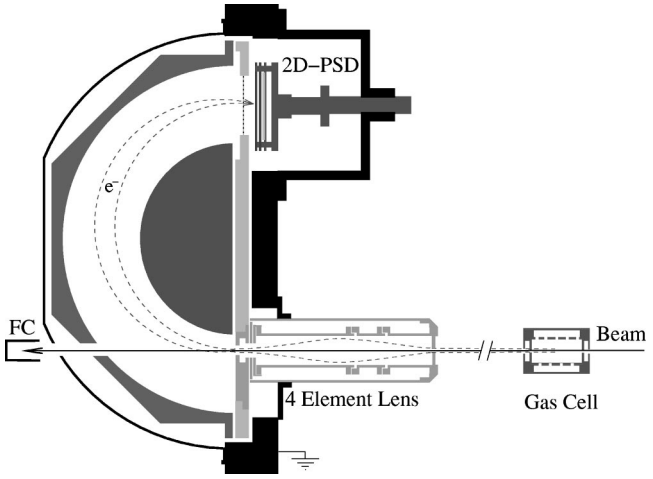

FIG. 1. The zero-degree Auger-electron spectrograph showing schematics of the gas cell, four-element lens, and hemispherical analyzer with a two-dimensional position sensitive detector (2D-PSD). The Faraday cup (FC) located at the exit of the spectrograph is used for normalization purposes.

The Ar gas target was maintained at constant pressure, utilizing a feedback-controlled baratron gauge. The target pressure was set at appropriate values to assure single collision conditions. Figure 2 shows the target pressure dependence of the Auger-electron emission from the *KLL* states of the 13 MeV C^{3+} ions. The number of detected electrons increases linearly with the target pressure in the range of 0–40 mTorr, while it decreases to zero when the gas flow is turned off. Consequently, the double collisions are still negligible up to Ar gas pressures of 40 mTorr.

Another potential source of an error is the possible beam

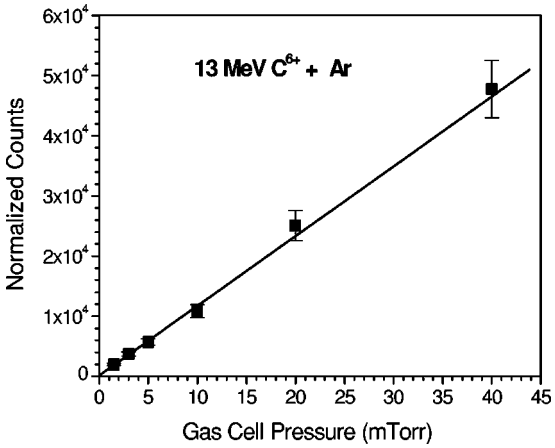

FIG. 2. Target pressure dependence for the *KLL* Auger electron emission in 13 MeV $C^{6+}+Ar$ collisions. The solid line represents the linear fit to the experimental data.

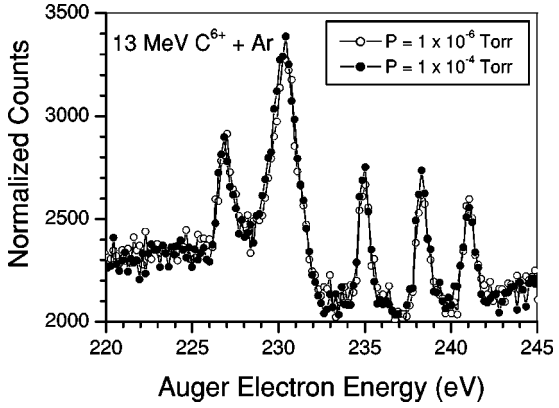

FIG. 3. 13 MeV $C^{6+}+Ar$ Auger-electron spectra measured with low and high vacuum pressure in the area between the analyzing magnet and the gas cell. Solid circles represent experimental data taken with a vacuum pressure of 1×10^{-4} Torr and open circles represent experimental data taken with a vacuum pressure of 1×10^{-6} Torr.

contamination with C^{5+} and C^{4+} ions. In this case, the *KLL* states of C^{3+} may be populated by single or double electron capture from the residual gas. Therefore, the effect of the vacuum pressure on the *KLL* Auger-electron emission was studied. The bare C^{6+} ions travel a distance of about 2 m after the analyzing magnet at a residual gas pressure of 1×10^{-6} Torr before entering the gas cell. To evaluate the contribution of a possible contamination, the vacuum pressure between the analyzing magnet and the gas cell was increased by a factor of 100, up to 1×10^{-4} Torr, and measurement of the Auger-electron emission from the *KLL* lines was repeated. Figure 3 shows two *KLL* spectra taken for the 13 MeV $C^{6+}+Ar$ collision system, normalized to the beam current. The open circles represent the data taken with the lower vacuum pressure of 1×10^{-6} Torr, and the solid circles represent the data taken with the higher vacuum pressure of 1×10^{-4} Torr. There are five peaks formed by an Auger decay of doubly excited *KLL* states of C^{3+} in the spectra. For both vacuum pressure settings the integrated *KLL* Auger-electron emission is the same. Therefore, the formation of C^{5+} or C^{4+} ions between the analyzing magnet and the gas cell that contribute to the population of *KLL* states is negligible. Consequently, the above study clearly showed that the observed doubly excited states of C^{3+} are formed in a single collision of C^{6+} ions with Ar.

III. THE INDEPENDENT-PARTICLE MODEL

Since the independent-particle model generally does not specify a certain treatment of the involved electrons, a brief description of its features, used in this study, is given. The screening dynamics of the incident projectile ion by captured target electrons play an important role in understanding multielectron processes in highly charged ion-atom collisions. In the case of high impact velocities, if several electrons are transferred during the collision, the projectile's energy levels will not fully readjust to reflect the dynamics of changes due to the insufficient interaction time. Therefore, the projectile charge will be only partly screened during the collision by the captured electrons. In order for the interaction time to be considered small, the impact velocity has to exceed the projectile's electron orbital velocity. In the investigated system, 6–13 MeV $C^{6+}+Ar$, impact velocities (4.5–6.6 a.u.) are greater than *K*- (4.2 a.u.) and *L*- (2.1 a.u.) shell velocities of C^{5+}. As mentioned above, the ECB model cannot be employed in this case since the collision time is not sufficient for target electrons to be molecularized. Instead, captured electrons should rather be treated as independent particles, captured by an unscreened potential. The total triple electron capture probability *P* is then a statistical product of single electron capture probabilities. The detailed calculation of *P* from single electron capture probabilities is presented at the end of this section.

The two-center semiclassical close-coupling method, based on an atomic orbital expansion, has been used to calculate single electron transfer probabilities. The method is found to be quite successful in explaining the state selective electron transfer cross sections at least for loosely bound outer shell electrons. The motion of the projectile is approximated by a classical trajectory and the target electrons are treated quantum mechanically. For treating electron capture from the inner shells, an independent electron model is used, and the active electron is described by a model potential fitted so that the binding energies of the inner-shell electrons are reproduced. Although the possible role of outer-shell electrons (the so-called Pauli exchange effect) is not included explicitly in the theory it may be partially accounted for in using a model potential.

Since the triple electron capture process is expected to have a very low cross section at high collision energies, the collision system should be optimized to increase the electron transfer probabilities. This can be achieved by matching the electron orbital velocities of the target and the projectile. In Fig. 4 the energy level diagram for C^{5+} and neutral Ar is shown. It is clearly seen that the binding energy for the Ar *L* shell is located between *K* and *L* shell energy levels of C^{5+}. Thus, the electron capture probability from the Ar *L* shell to the *K* and *L* shells of C^{5+} is enhanced. At the same time, the contribution from *K* and *M* shells to the total capture is significantly reduced, as can be seen from the work of Rødbro *et al.* [20], where contributions from *K*, *L*, and *M* shells of Ar into the total single electron capture cross sections are compared for fast proton on Ar collisions. In addition, the Nikolaev Oppenheimer-Brinkman-Kramers approximation [21] was used in this study to estimate the relative influence of capture probabilities from the *K*, *L*, and *M* shells of Ar numerically. It was shown that, for the investigated collision energy range of 0.5–1.1 MeV/u, the *K* shell contributes less than 0.01% and the *M* shell contributes about 0.5% to the total capture. Therefore, target electrons are mainly captured from the *L* shell and transfer probabilities from *K* and *M* shells of Ar are negligible.

The *L* shell of Ar consists of three energetically resolved sublevels (*nlm*), recognized in the nonrelativistic close-coupling code as $2s0$, $2p0$, and $2p\pm1$, filled with two, two, and four electrons, respectively. Out of these eight electrons, one is captured to the *K* shell ($1s0$) of C^{5+} and two others

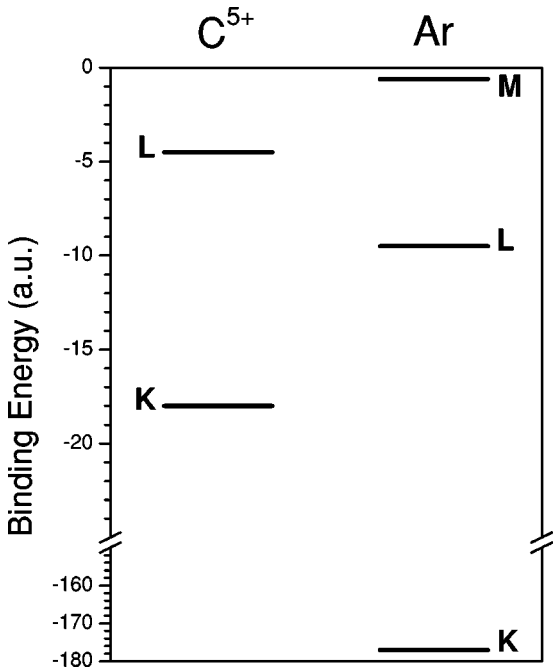

FIG. 4. The energy level diagram for the $C^{6+}+Ar$ collision system. *K* and *L* shell binding energies of C^{5+} match the *L* shell binding energy of Ar, which maximizes the electron transfer probability.

are captured to the *L* shell $(2s0,\ 2p0,\ 2p\pm1)$. If C^j is the number of possible ways for any three electrons from the *L* shell of Ar in a certain electron configuration *j* to be captured to the *KLL* state in carbon, then the total triple electron capture probability can be expressed as

$$P(b)=\sum_j C^j \prod_{i=1}^{3} P_i^{kj}(b) \prod_{i=4}^{8} Q_i^j(b), \qquad (1)$$

where *j* is the sum over possible statistical configurations. P_i^{kj} is the probability for the *i*th electron of Ar in the *j* level $(2s0,\ 2p0,\ 2p\pm1)$ to be transferred to the *k* level (*K* or *L* shells) of C^{5+}. Q_i^j is the probability for the *i*th electron of Ar in the *j* level not to be transferred to either the *K* or *L* shell of C^{5+}.

IV. RESULTS AND DISCUSSION

Figure 5 shows the Auger-electron spectrum measured in collisions of 13 MeV C^{6+} ions with Ar gas targets. The formation of the $C^{3+}(1s2l2l')$ doubly excited states, namely, $1s2s^2\ ^2S$, $1s2s2p\ ^4P$, $[1s(2s2p)^3P]\ ^2P_-$, $[1s(2s2p)^1P]\ ^2P_+$, and $1s2p^2\ ^2D$, which Auger decay to the $C^{4+}(1s^2)$ ground state, is prominent. All the above states were populated by triple capture, which allows for the population of all possible Li-like doubly excited states. Therefore the $^2S, ^2P$, and ^4P states corresponding to the $1s2p^2$ configuration are also populated. However, the ^2P and ^4P states are not allowed to Auger decay to the $C^{4+}(1s^2)$ ground state due to parity conservation considerations, while the ^2S state has a very low Auger decay rate to be observed.

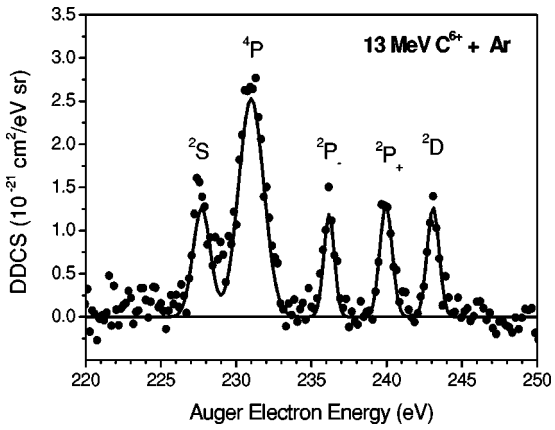

FIG. 5. Absolute Auger-electron DDCS spectra for the collision system of 13 MeV $C^{6+}+Ar$, recorded at zero degrees with respect to the beam direction. The formation of the $C^{3+}(1s2l2l')\ ^2S, ^4P, ^2P_-, ^2P_+$, and ^2D doubly excited states by triple electron capture, which Auger decay to the $C^{4+}(1s^2)$ ground state, is prominent. Note that the larger width of the ^4P peak is due to spectroscopic considerations (see discussion in Sec. IV). The solid line represents the Gaussian fit to the experimental data.

In order to determine the experimental SCDS for the population of the Li-like doubly excited states via triple capture, the area under the peaks was obtained after fitting the DDCS data with Gaussian distributions, as can be seen in Fig. 5. The integrated area was then converted to SDCS's after accounting for certain corrections, as discussed below.

First, in order to correct the experimental cross sections for the x-ray decay channel, undetectable in this study, the Auger yields *Y* for the observed transitions were evaluated from theoretical autoionization and fluorescence rates [22–24]. Also, the decay path of the long-lived $1s2s2p\ ^4P$ state was taken into account. It is a metastable state, with lifetimes of 25 ns for $J=5/2$, 9.1 ns for $J=3/2$, and 3.0 ns for $J=1/2$ [23,25], which are in general comparable to the ion's time of flight in the gas cell (e.g., in the case of 13 MeV C^{6+}, TOF=3.5 ns). However, due to the spectrograph geometry, electrons emitted in the area between the gas cell and the analyzer entrance (see Fig. 1) will still be recorded, thus enhancing the electron yield of the state but also decreasing the energy resolution of the line, as is observed in Fig. 5. The correct electron yield for the $1s2s2p\ ^4P$ state was obtained after biasing the gas cell by a voltage of -30 V, which energetically separates the yield fractions originating from inside and outside the gas cell area. The total electron yield was then calculated from the available ion's time of flight and the exponential decay rate of the state [26]. The above corrections were included in the same factor *R* for each collision energy. Finally, the four doubly excited states $^2D, ^2P, ^4P$, and ^2S belonging to the same electron configuration $1s2p^2$ were populated by triple capture according to their statistical weight. However, since only the ^2D state is observed, as discussed earlier, the production of other states was accounted for as shown by the inverse term in Eq. (2).

With the above considerations the single differential cross section for the triple electron capture to the *KLL* states of C^{3+} is given by

TABLE I. Correction factors for the extraction of the experimental SDCS's for the triple electron capture to the C^{3+} *KLL* states, from the corresponding DDCS spectra. SDCS's calculated within the independent-particle model are also given. *Y* is the Auger yield, and *R* is the correction factor accounting for the lifetimes of the intermediate states. Transition energies are given relative to the $C^{4+}(1s^2)$ ground state in units of eV. Both experimental and calculated SDCS's are in units of 10^{-21} cm^2/sr. All data are referred to the case of the 13 MeV $C^{6+}+Ar$ collision system.

Intermediate state	Transition energy	Integrated peak area	*Y*	*R*	Statistical weight	SDCS Expt.	SDCS Calc.
$1s2s^2\ ^2S$	227.5 [a]	1.8±0.6	≃1 [b]	1.00	1	1.8±0.6	
$1s2s2p\ ^4P$	229.7 [a]	5.3±1.6	≃1 [c]	0.51	1	10.5±3.2	
$1s2s2p\ ^2P_-$	235.9 [a]	1.1±0.5	0.92 [d]	1.00	1	1.1±0.3	
$1s2s2p\ ^2P_+$	239.3 [a]	1.3±0.4	≃1 [d]	1.00	1	1.3±0.4	
$1s2p^2\ ^2D$	242.3 [a]	1.3±0.4	≃1 [b]	1.00	3	3.8±1.1	
					SDCS(sum)	18.6±0.6	30.6

[a]From Ref. [27].
[b]Assumed 1 based on Ref. [24].
[c]From Ref. [23].
[d]From Ref. [22].

$$\left(\frac{d\sigma}{d\Omega}\right)=\sum_i\left(\frac{d\sigma}{d\Omega}\right)^i=\sum_i Z^i_{exp}\ \frac{1}{Y^i_A}\ \frac{1}{R^i}\left[\frac{2J+1}{\sum_J(2J+1)}\right]^{-1}, \tag{2}$$

where *i* is the sum over the observed *KLL* doubly excited states. In Table I, the discussed correction factors are presented for the 13 MeV $C^{6+}+Ar$ collision system.

The triple electron capture probability $P(b)$ was obtained within the independent-particle model as given by Eq. (1). The total triple electron capture cross section σ was then determined after integrating the probability $P(b)$ over the impact parameter, i.e.,

$$\sigma = 2\pi\int_0^\infty P(b)bdb. \tag{3}$$

In order to compare the independent-particle model calculations with the experimental zero-degree SDCS, the total cross section σ was differentiated with respect to the solid angle assuming an isotropic distribution for the *KLL* Auger electrons. Thus, the calculated zero-degree SDCS for the triple electron capture to *KLL* states is finally expressed as

$$\frac{d\sigma(\theta=0°)}{d\Omega}=\frac{\sigma}{4\pi}. \tag{4}$$

In Fig. 6 the experimental zero-degree triple electron capture cross sections to *KLL* states measured for 6, 9, and 13 MeV $C^{6+}+Ar$ collisions are compared with the independent-particle model calculations for the corresponding collision energies. The experimental error bars are calculated by taking the quadrature sum of the statistical and absolute uncertainties. The latter incorporates mainly the electron detection efficiency of the spectrograph.

It is seen clearly from Fig. 6 that the independent-particle model calculations systematically overestimate the experimental triple capture SDCS's by a factor of about 1.5. The predicted collision energy dependence of the process is in good agreement with the experimental one. Considering the fact that the theoretical single electron capture amplitudes contain some uncertainty not shown in Fig. 6, the comparison gives enough evidence to conclude that the independent-particle model provides an adequate description of the triple electron capture in fast ion-atom collisions, therefore validating physical ideas incorporated in the model. Specifically, the screening dynamics of the incident projectile ion by captured target electrons can be understood through simultaneous electron transfer, in which the energy levels of the projectile do not completely readjust during the course of the collision due to the insufficient interaction time. Therefore, if the impact velocity exceeds the projectile electron orbital veloci-

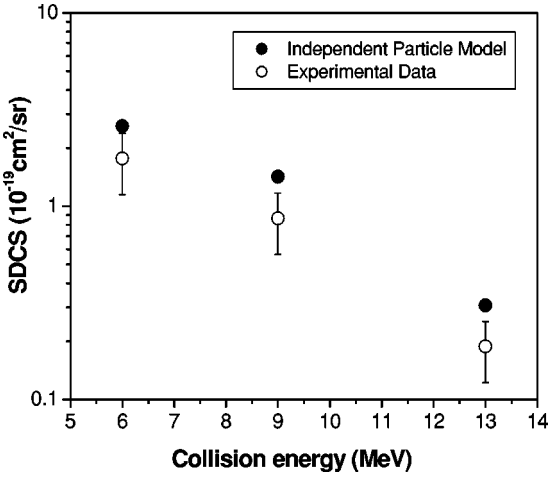

FIG. 6. Absolute SDCS measurements of triple electron capture to the C^{3+} *KLL* states, populated in fast collisions of bare carbon ions with Ar targets (open circles). Independent-particle model calculations (solid circles) are seen to be in fairly good agreement with the data.

ties, the ion nucleus remains essentially unscreened during the collision. In addition, since the independent-particle model does not account for the electron-electron correlation explicitly, the role of the electron-electron correlation in triple electron capture by fast ions is believed to be not as significant as in slow collisions [13].

V. CONCLUSIONS

Zero-degree Auger-electron spectroscopy has been used to determine the absolute single differential cross sections for triple electron capture to doubly excited *KLL* states of carbon in collisions of fast ($v = 4.5$–6.6 a.u.) C^{6+} ions with Ar atoms. Experimental data were used to test the predictions of the independent-particle model that utilizes single electron capture probabilities calculated using the two-center semiclassical close-coupling method, based on an atomic orbital expansion. Single differential cross sections were obtained from the total cross section calculations after assuming an isotropic Auger emission. Model calculations were found to be in fairly good agreement with the experiment, signifying that the independent-particle model provides an adequate description of the triple electron capture in fast ion-atom collisions. In particular, it was concluded that target electrons are captured simultaneously by an essentially unscreened potential of the projectile, reflecting the fact that the collision time is small for ion energy levels to readjust. The effects of electron-electron correlation do not appear to be significant in multiple electron transfer at high collision velocities.

ACKNOWLEDGMENTS

This work was supported by the Division of Chemical Sciences, Geosciences and Biosciences, Office of Basic Energy Sciences, Office of Science, U.S. Department of Energy. The authors would like to acknowledge insightful discussions with C. L. Cocke.

[1] J. Vancura, J.J. Perotti, J. Flifr, and V.O. Kostroun, Phys. Rev. A **49**, 2515 (1994).
[2] R. Ali, C.L. Cocke, M.L.A. Raphaelian, and M. Stöckli, Phys. Rev. A **49**, 3586 (1994).
[3] N. Nakamura *et al.* J. Phys. B **28**, 2959 (1995).
[4] N. Selberg, C. Biedermann, and H. Cederquist, Phys. Rev. A **56**, 4623 (1997).
[5] S. Martin *et al.* Phys. Rev. Lett. **77**, 4306 (1996).
[6] J.H. Posthumus and R. Morgenstern, Phys. Rev. Lett. **68**, 1315 (1992).
[7] J.H. Posthumus and R. Morgenstern, J. Phys. B **25**, 4533 (1992).
[8] H. Merabet *et al.* Phys. Rev. A **59**, R3158 (1999).
[9] E.D. Emmons, A.A. Hasan, and R. Ali, Phys. Rev. A **60**, 4616 (1999).
[10] H. Ryufuku, K. Sasaki, and T. Watanabe, Phys. Rev. A **21**, 745 (1980).
[11] A. Barany *et al.*, Nucl. Instrum. Methods Phys. Res. B **9**, 397 (1985).
[12] H. Niehaus, J. Phys. B **19**, 2925 (1986).
[13] H. Zhang *et al.*, Phys. Rev. A **64**, 012715 (2001).
[14] T.C. Theisen and J.H. McGuire, Phys. Rev. A **20**, 1406 (1979).
[15] J. Kuang and C.D. Lin, J. Phys. B **29**, 1207 (1996).
[16] D.R. Bates and R. McCarrol, Proc. Phys. Soc., London, Sect. A **245**, 175 (1958).
[17] E.P. Benis *et al.*, Nucl. Instrum. Methods Phys. Res. B **146**, 120 (1998).
[18] E.P. Benis, T.J.M. Zouros, and P. Richard, Nucl. Instrum. Methods Phys. Res. B **154**, 276 (1999).
[19] E.P. Benis, T.J.M. Zouros, H. Aliabadi, and P. Richard, Phys. Scr., T **T80B**, 529 (1999).
[20] M. Rødbro, E.H. Pedersen, C.L. Cocke, and J.R. Macdonald, Phys. Rev. A **19**, 1936 (1979).
[21] V.S. Nikolaev, Sov. Phys. JETP **24**, 847 (1967).
[22] M.H. Chen, B. Crasemann, and H. Mark, Phys. Rev. A **27**, 544 (1983).
[23] B.F. Davis and K.T. Chung, Phys. Rev. A **39**, 3942 (1989).
[24] D.H. Lee *et al.*, Phys. Rev. A **44**, 1636 (1991).
[25] B.F. Davis and K.T. Chung, Phys. Rev. A **36**, 1948 (1987).
[26] M. Zamkov *et al.*, Phys. Rev. A **64**, 052702 (2001).
[27] M. Rødbro, R. Bruch, and P. Bisgaard, J. Phys. B **12**, 2413 (1979).